

## Article

# Energy and Economic Sustainability of a Trigeneration Solar System Using Radiative Cooling in Mediterranean Climate

Marco Noro <sup>1,\*</sup> , Simone Mancin <sup>1</sup> and Roger Riehl <sup>2</sup> 

<sup>1</sup> Department of Management and Engineering, University of Padova, 36100 Vicenza, Italy; simone.mancin@unipd.it

<sup>2</sup> National Institute for Space Research, São José dos Campos 12227-010, SP, Brazil; roger.riehl@gts.com.br

\* Correspondence: marco.noro@unipd.it

**Abstract:** The spreading of nearly zero-energy buildings in Mediterranean climate can be supported by the suitable coupling of traditional solar heating, photovoltaics and radiative cooling. The latter is a well-known passive cooling technique, but it is not so commonly used due to low power density and long payback periods. In this study, the energy performance of a system converting solar energy into electricity and heat during the daytime and offering cooling energy at night is assessed on the basis of a validated model of a trifunctional photovoltaic–thermal–radiative cooling module. The key energy, CO<sub>2</sub> emission and economic performance indicators were analyzed by varying the main parameters of the system, such as the spectral emissivity of the selective absorber plate and cover and thermal insulation thickness. The annual performance analysis is performed by a transient simulation model for a typical residential building and two different climates of the Mediterranean area (Trapani and Milano). For both climates, glass-PVT–RC is the best solution in terms of both overall efficiency (electric + thermal) and cooling energy capacity, even better with a thicker insulation layer; the annual electrical, heat and cooling gains of this system are 1676, 10,238 and 3200 kWh for Trapani, correspondingly (1272, 9740 and 4234 kWh for Milano, respectively). The typical glass-PVT module achieves a performance quite similar to the best ones.

**Keywords:** cogeneration; Mediterranean climate; photovoltaic/thermal; radiative cooling



**Citation:** Noro, M.; Mancin, S.; Riehl, R. Energy and Economic Sustainability of a Trigeneration Solar System Using Radiative Cooling in Mediterranean Climate. *Sustainability* **2021**, *13*, 11446. <https://doi.org/10.3390/su132011446>

Academic Editor: Domenico Mazzeo

Received: 20 September 2021

Accepted: 14 October 2021

Published: 16 October 2021

**Publisher's Note:** MDPI stays neutral with regard to jurisdictional claims in published maps and institutional affiliations.



**Copyright:** © 2021 by the authors. Licensee MDPI, Basel, Switzerland. This article is an open access article distributed under the terms and conditions of the Creative Commons Attribution (CC BY) license (<https://creativecommons.org/licenses/by/4.0/>).

## 1. Introduction

Even if the extensive application of insulation is reducing the energy demand for new and refurbished buildings, the heating demand remains high in more commonly diffused existing buildings, particularly in temperate zones [1]. On the other hand, the cooling energy demand is increasing especially in milder climates, due to global climate change and to the reduced capacity of more insulated buildings to waste energy [2]. In the last decades, more efficient heating and cooling systems have become desirable to reduce the conventional energy demand from fossil fuels or electricity, such as condensing boilers, heat pumps, open and closed cycle sorption systems, solar thermal and electrical technologies.

Nowadays, solar energy is considered the most promising renewable energy in the world, despite it not being the most widely used [3]. The most widespread solar technologies are solar thermal collectors (that produce hot water or air) and photovoltaic (PV) modules (that produce electricity). According to [4], at the end of 2020, the cumulative PV installed power was 137.2 GW in the European Union, with an annual gross electricity production of 145.9 GWh (i.e., 5.3% share). As it is well known, the thermal efficiency of a solar thermal collector highly depends on its photothermal conversion efficiency and heat loss [5]. In particular, it relies on its spectral absorptivity in the solar heating (SH) band (0.2–3 μm) and on the radiative heat loss in the middle- and far-infrared band (>3 μm). Starting from the beginning of this century, a series of improvements regarding solar thermal collectors have been proposed. Higher performance selective coatings were developed, with an absorptivity of approximately 0.95 and an emissivity as low as 0.05 [6,7]. Thus, a

first-order thermal loss coefficient of  $1 \text{ W m}^{-2} \text{ K}^{-1}$  or even less is now the standard value in the solar thermal collectors largely available on the market.

Concerning the solar conversion to electricity, not all wavelengths of the incoming radiation are usefully converted into electricity in PV cells; commercially available single-junction PV cells have an electrical efficiency varying between 6% and 25% (under optimum operating conditions and depending on the semiconductor material), whereas the rest of the solar radiation is dissipated as heat [4,8]. This is due to the band-gap energy of the semiconductor material. For example, crystalline silicon PV cells can utilize the entire visible spectrum plus some part of the infrared spectrum. The energy of all other wavelengths (far-infrared and higher energy radiation) cannot be converted into electricity; unfortunately, it is dissipated by the cell as thermal energy. The main drawback is that the PV module can reach temperatures as high as  $40 \text{ }^\circ\text{C}$  above ambient; this causes an increased intrinsic carrier concentration which tends to increase the dark saturation current of the p–n junction. The main effect is the decreasing of the available maximum electrical power, typically 0.2–0.5% for every  $1 \text{ }^\circ\text{C}$  rise in the PV module temperature for crystalline silicon cells. Another critical issue for improving the performance of PV systems is maintaining a homogeneous low-temperature distribution across the string of cells.

The well-known main idea to face these issues is to increase the electrical production of PV by decreasing the normal operating cell temperature; this can be performed by cooling the panel with a liquid (or air). Thus, photovoltaic/thermal technology (PVT) aims at using the same collector area for producing both electricity and heat. This also implies to have higher global efficiency with enhanced use of solar incoming energy [9,10].

Besides the direct conversion of solar radiation into thermal and electrical energy, solar thermal cooling was one of the first studied technologies in the aftermath of the 1973 energy crisis relative to the cooling of buildings. Despite many successful pilot plants, this technology has not taken off yet. Over and over, intergovernmental organizations [3] or multi-stakeholder governance groups [11] have recommended the development of solar cooling. The fact is that the last recording of installations worldwide reached only 1200 plants in 2014, most of them in Europe [12]. The system appears expensive and complex. Moreover, in temperate climates, the ab/adsorption chiller is utilized only in summer, so the investment costs are even less advisable. Furthermore, the progressive cost reduction of PV panels that occurred in the first decade of the present century allows a possible competition between solar PV cooling systems to occur, where PV panels drive a compression chiller. The further impressive PV price reduction of the last decade seems to definitively close the game; now, the competition of solar electrical cooling in terms of the overall cost is rather against conventional air-conditioning [13]. Nevertheless, some recent studies have highlighted an interesting energy performance based on dynamic simulations of solar cooling plants coupling evacuated tube collectors with ground source heat pumps [14], also using PVT modules [15].

Radiative cooling (RC) can be considered a viable alternative to solar thermal and solar PV cooling. It is a renewable energy technology that uses the high spectral transmittance of the atmosphere in the so-called “atmospheric window” band ( $8\text{--}13 \text{ }\mu\text{m}$ , also called the “RC band”) to extract heat from a collector by radiative heat exchange with cold outer space [16–18].

The cooling performance of a radiative cooler is positively affected by the clearness of the atmosphere and the spectral emissivity in the RC band of the cooling surface. In fact, the cooling surface should have the lowest possible spectral absorptivity (that is, emissivity) in the bands excluding the RC band to maintain the surface temperature as low as possible. In the last years, daytime RC has also been successfully achieved thanks to the development of materials science in the micro–nano scales that allows researchers to further strengthen the spectral selectivity of RC coatings [19,20].

The spectral selectivity of the SH coating and that of the RC coating are incompatible; the former features extremely low emissivity in the middle- and far-infrared bands, particularly the RC band, while the latter features low absorptivity in the SH band. As

a consequence, solar collectors can be used only during the daytime, when most of the radiative coolers normally cannot run. Furthermore, the solar heat collectors are more useful in spring, autumn and winter, when the RC collectors' value is minor, compared with its summer value. Finally, the RC collector shows a cooling power density lower than the vapor compression refrigeration system, in the range of 40–80 W m<sup>-2</sup>; thus, the payback period of SH and RC systems is long due to all these characteristics.

For such reasons, it is worth analyzing the system setup by integrated diurnal solar thermal and photovoltaic (PVT) and nightly RC functions with one single collector. Such a system would extend the operation time of conventional solar installations until nighttime, while eliminating the cost disadvantages of stand-alone RC collectors. Moreover, it would feature an increased overall efficiency and seasonal adaptability.

Some authors have already studied SH–RC systems. Chen and Lu recently have published a comprehensive review on radiative cooling and its integration within buildings [21]. Furthermore, in [22], studies on the influence of cover shield on radiative cooling are reported. Material properties and application performance are summarized according to the spectral selectivity, also referring to SH. Nevertheless, only a group of authors developed a mathematical model that considers the spectral radiant distribution of the coating and atmosphere [23–27]. Numerical calculations were performed to investigate the heating and cooling performance of the hypothetical spectrally selective SH–RC surface by comparing it with three other typical surfaces. They also investigated a trifunctional photovoltaic–photothermic–radiative cooling (PVT–RC) collector and a practical-scale testing system was built to verify the effectiveness of the numerical model [28–30].

In all those studies, the authors investigated numerically and experimentally some key performance indicators of the system, such as its diurnal thermal efficiency under different ambient temperatures, inlet temperature and solar irradiance. The nocturnal cooling power under different inlet temperatures and sky conditions was investigated as well. Surfaces with different spectral selectivity were also tested. However, only a parametric analysis of the PVT–RC and SH–RC collectors was made and no annual energy performance of the whole system was evaluated.

The originality of the present study is the simulation by Trnsys® of the annual performance of the system, based on the mathematical model of the PVT–RC module, to face the loads (heating, cooling, domestic hot water (DHW) and electricity) of a residential building. The annual performance of the hybrid trigeneration system is evaluated to investigate its electricity, heat and cooling energy outputs, efficiency and load factor, both in specific and total terms. The simulations are run in two different typical Mediterranean climates to analyze the effect on the system performance. To quantify the effect on energy performance, such analysis is carried out by varying different key structural parameters of the collector, such as cover emissivity, collector plate emissivity and thermal insulation thickness. The environmental and economic viability of different configurations of the proposed trigeneration solution are also evaluated.

## 2. Materials and Methods

### 2.1. Energy Needs of the Building

To evaluate the sustainability of the proposed trigeneration system from the energy, CO<sub>2</sub> emission and economic point of view, a model of a residential building was realized [31]. Dynamic simulations by Trnsys® were performed to determine the heating and cooling demand data. The single-family detached house here considered had two floors (area of 77 m<sup>2</sup> and 58 m<sup>2</sup>, respectively) and a total volume of 363.5 m<sup>3</sup>. The main entrance had an orientation to the north and the portico to the south; a wall of the living room was oriented to the west.

A free tool of Trnsys® called the domestic hot water load profile generator was used to generate a DHW load profile consumption, with a daily DHW demand of approximately 200 L at 40 °C. The data for the electricity demand in terms of average hourly electrical consumption of a household for the main uses (fridges and freezer, lighting, dishwasher

and washing machine, multimedia tools) were taken from [31]. The analyses regarding two resorts representative of very different Mediterranean climates were performed according to the Koppen classification for which Test Reference Years [32] are available, namely, Milano (Italy, 45.5° N), for the Cfa climate (temperate and humid in all seasons climate with a hot summer—the hottest month has a mean temperature greater than 22 °C), and Trapani (Italy, 38° N), for the Csa climate (temperate with dry summer climate with a hot summer—the hottest month has a mean temperature above 22 °C). The annual total energy demands for the house located in Trapani (TR) for space heating, DHW, cooling and electricity were determined to be approximately 2860 kWh, 2727 kWh, 2008 kWh and 2120 kWh, respectively. The same figures for Milano (MI) were 9452 kWh, 2727 kWh, 505 kWh and 2120 kWh, respectively (Figure 1).

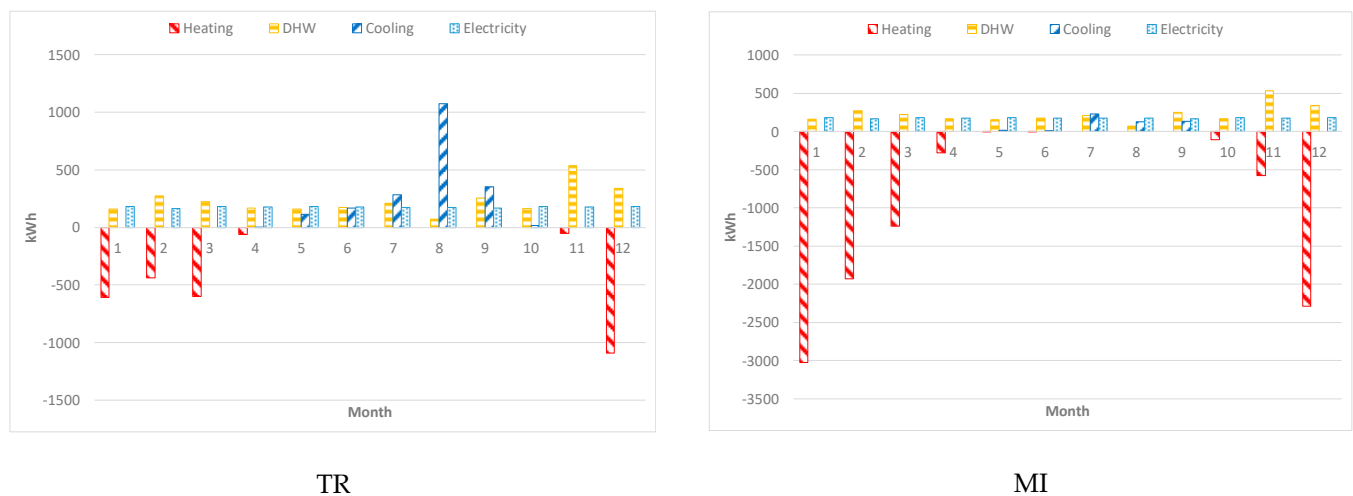


**Figure 1.** Heating, cooling, DHW and electricity energy needs for the residential building located in Trapani (TR) and Milano (MI).

## 2.2. Spectral Characteristics of The Collectors

In this study, three surfaces with different spectral characteristics in terms of absorptivity (i.e., emissivity) for the collector plate are considered. Furthermore, two surfaces with different spectral characteristics in terms of transmittance for the cover are also considered (Figure 2). The main scope is to perform a comparison of the solar trigeneration system in different cases from the energy performance, environmental sustainability and economic viability points of view. The combination of three collector plates and two covers provides six different configurations.

Figure 2 reports the spectral emissivity of a typical PVT collector (high spectral absorptivity in the SH band and low values otherwise, yellow continuous line), a typical radiative cooler (high spectral emissivity in the RC band and low values otherwise, dotted blue line) and a PVT–RC collector with high spectral absorptivity (i.e., spectral emissivity) in the SH and RC bands (hatched purple line). The values that we consider in this study are the following:

- a spectrally selective PVT–RC surface with an average absorptivity of 0.92 in the SH band, i.e., nearly the same as that of the real SH surface;
- an average emissivity of 0.70 in the RC band, i.e., nearly the same as that of the real RC surface, and an average absorptivity (emissivity) of 0.05 in other bands, i.e. nearly the same as that of the real SH surface.

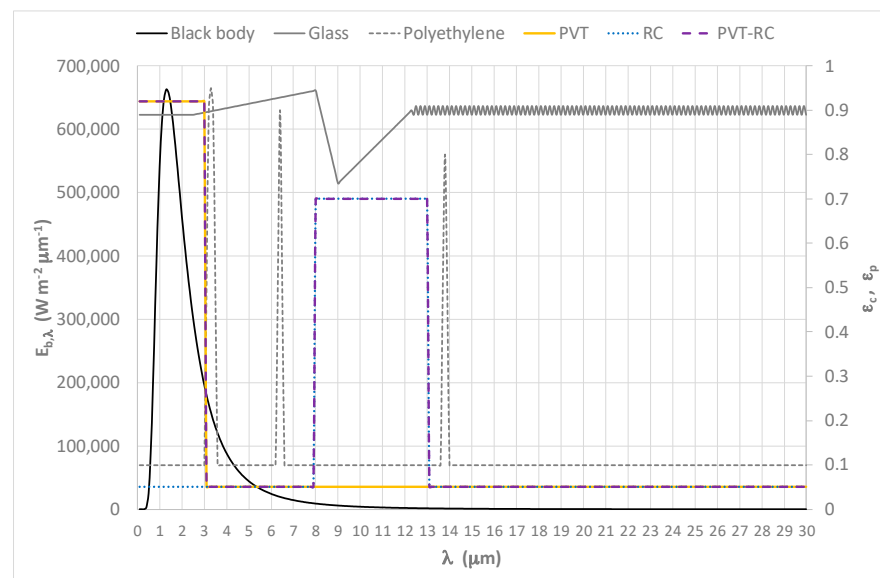


**Figure 2.** Spectral properties of the black body (spectral radiation power  $E_{b,\lambda}$  at 2200 K, left y axis), of the collector plate (PVT, RC and PVT-RC) and the transparent cover (glass, polyethylene) (emissivity  $\epsilon_p$  and  $\epsilon_c$ , respectively, right y axis) [27–30].

Concerning the transparent cover, the polyethylene film is commonly applied on the RC thanks to its high transmissivity in most bands, particularly in the RC band. As a drawback, it has low mechanical resistance to adverse meteorological phenomena [25]. Conversely, the glazing acts as the cover in PVT collectors, but it is not properly suitable for RC as it is “opaque” to the mid-and long-wave infrared radiation. In the present study, both a 6  $\mu\text{m}$  thick polyethylene film and a 2.8 mm thick glass served as the cover of the different collectors considered. In fact, even if the direct heat exchange between the plate and the cold sky is inhibited when using glass, the plate can firstly dissipate heat to the glass cover by heat radiation and convection and then the glass cover exchanges heat to the sky by radiative cooling. The high long-wave absorptivity and emissivity on both sides of the glass cover allow the PVT collector to feature a quite effective cooling capacity. This can be considered as an additional bonus of PVT, so a lower cooling performance concerning the modified polyethylene film-based PVT-RC collector is acceptable. The transmittance characteristics of both the low-density polyethylene film and the glass are reported as absorptivity (i.e., the complement to one of the transmittances assuming a very low reflection coefficient of 0.01) in Figure 2.

### 2.3. The Trigeneration Solar System

As depicted in Figure 3, the modelled collectors had a flat-plate structure, with overall dimensions of 2000 mm  $\times$  1000 mm  $\times$  80 mm. The baseplate in aluminum presented the dimensions of 1964 mm  $\times$  964 mm  $\times$  0.4 mm; it was fully covered by a 0.3 mm thick layer of black Tedlar–polyester–Tedlar (TPT). On the latter, 72 mono-crystalline silicon PV cells, with an area of 1.12 m<sup>2</sup>, were laminated in PVT cases. An encapsulation layer of transparent TPT was placed above the PV cells and the black TPT. Two glue layers of ethylene–vinyl–acetate (EVA) were fixed between the aluminum plate and the TPTs. A 40 mm high air gap was set between the cover and the plate. Seven water copper tubes, each with an inner diameter of 8 mm and an external diameter of 10 mm, were welded in parallel at the backside of the aluminum plate. A 40 mm thick layer of glass fiber was adopted as the back insulator of the collector.

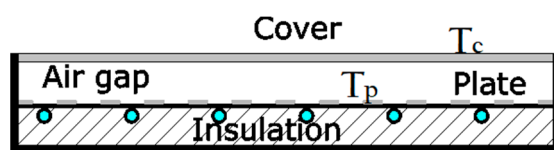


**Figure 3.** Cross-section view of the collector. The cover can be glass or polyethylene, the plate can be with PVT, RC, or PVT-RC spectral characteristics.

The collector was placed with an unobstructed view of the sky and it was set to a tilt angle suitable to optimize the solar radiation collection during the year ( $27.9^\circ$  in Trapani,  $35.5^\circ$  in Milano). A simplified schematic of the plant is reported in Figure 4, where only the heating energy is reported. Here, the collectors (primary circuit) were connected to the building loads (secondary circuit) by a de-coupler (heat exchanger), whose efficiency was fixed and supposed constant. The main variables are reported in Table 1. The complete description of the mathematical model of the collector is described in the full references [23–30].

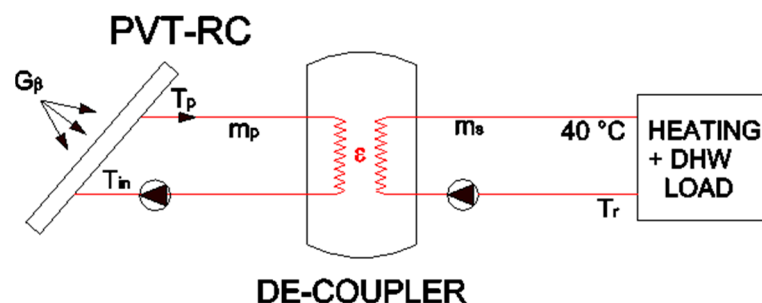


**Figure 4.** Simplified functional diagram of the solar plant (only heating energy is reported).

**Table 1.** Values of the main variables of Figure 4.

Variable (Unit)	Value
Primary circuit specific mass flow rate ( $m_p$ ) ( $\text{kg h}^{-1} \text{m}^{-2}$ )	60
Secondary circuit specific mass flow rate ( $m_s$ ) ( $\text{kg h}^{-1} \text{m}^{-2}$ )	20
Collector area ( $\text{m}^2$ )	10
Distance of cover-plate ( $d_{p,c}$ ) (mm)	40
Insulation thickness ( $d_b$ ) (mm)	40
Insulation thermal conductivity ( $k_b$ ) ( $\text{W m}^{-1} \text{K}^{-1}$ )	0.04
Reflectance of cover ( $\rho_c$ )	0.01
Reflectance of plate ( $\rho_p$ )	0.10
Transmittance ( $\tau_c$ )—Polyethylene	0.90
Transmittance ( $\tau_c$ )—Glass mid-and far-infrared (night)	0.10
Transmittance ( $\tau_c$ )—Glass near infrared (day)	0.90
Reference electrical efficiency of the solar cells ( $\eta_{ref}$ )	16.0%
Temperature coefficient of the solar cells ( $B_r$ ) ( $\text{K}^{-1}$ )	0.0045
Efficiency of the heat exchanger ( $\epsilon$ )	0.8

#### 2.4. Hypotheses of The Analyses

The energy, environmental and economic analyses of the different collector configurations were performed in terms of the following:

- monthly energy production by the collector (electricity ( $E_{PVT}$ ), thermal energy ( $Q_{out,heat}$ ) and cooling energy ( $Q_{out,cool}$ )), both specific (per square meter of collector surface) and total values (for  $10 \text{ m}^2$  of collectors' area as reported in Table 1);
- monthly thermal ( $\eta_{th}$ ) and electrical ( $\eta_{el}$ ) efficiency, defined as the ratio between the useful energy produced by the collector and the global solar radiation  $G_\beta$  on the collector surface (Equation (1)):

$$\eta_{th} = \frac{Q_{out,heat}}{G_{\beta}} \quad \eta_{el} = \frac{E_{PVT}}{G_{\beta}} \quad (1)$$

- load factors (*LF*), that is, the ratio between the useful energy produced by the collector (electric, thermal and cooling) and the respective load of the building (Equation (2)):

$$LF_{el} = \frac{E_{PVT}}{E_{load}} \quad LF_{heat} = \frac{Q_{out,heat}}{Q_{heating+DHW}} \quad LF_{cool} = \frac{Q_{out,cool}}{Q_{cooling}} \quad (2)$$

- specific non-renewable primary energy (*PE*) consumed to satisfy the (possible) parts of the loads not fully covered by the collectors;
- non-renewable primary energy saving (*PES*) with respect to a reference traditional solution (natural gas-fired condensing boiler, air–water electric vapor compression chiller and electricity from the grid). To conduct such a comparison, reference efficiencies were fixed for electricity ( $\eta_{el,sp} = 51.3\%$ ) and thermal energy ( $\eta_{th,sp} = 95.2\%$ ) of the separate production on the base of the primary energy factors as defined by Italian Decree DM 26/06/2015, namely,  $f_{p,nren}$  (natural gas) = 1.05 and  $f_{p,nren}$  (electricity from the grid) = 1.95. An energy efficiency ratio of 3 was set for the cooling energy production by the conventional air–water chiller;
- CO<sub>2</sub> specific savings with respect to the traditional solution. Official data in Italy [33] were assumed for electricity (0.4 kgCO<sub>2</sub> kWh<sub>el</sub><sup>−1</sup>, which considers the mix of thermo-electric generating technologies, not including renewable sources such as hydro and photovoltaic plants) and for the natural gas boiler (0.2 kgCO<sub>2</sub> kWh<sup>−1</sup> of primary energy);
- the six configurations were compared to investigate the best solution from the economic point of view, i.e., with the maximum differential net present worth (*NPW*) and/or minimum discounted payback period (*DPP*). In this case, the *NPW* is defined on the basis of a time series of cumulative differential cash flows, i.e., it is calculated as the sum of the present values of the differential cash flows (*DCF*) of each solution, with respect to the traditional one, given the interest rate (2% in this study) and the period of the analysis (15 years) (Equation (3)). The *DPP* is the period of time required for the return on the investment in solar trigeneration to “repay” (by economic savings *S*) the sum of the original extra-investment *P* related to the traditional solution (Equation (4)) [34]:

$$NPW = \sum_{t=0}^{10} \frac{DCF_t}{(1 + 0.02)^t} \left[ \frac{\text{€}}{l/s} \right] \quad (3)$$

$$DPP = \frac{\log \frac{S}{(S-P \cdot 0.02)}}{\log(1 + 0.02)} [y] \quad (4)$$

To make the study more comprehensive, the analysis was conducted by varying the extra-investment *P* in a suitable range, here considered from EUR 1000 to EUR 4000. Concerning the operative costs, natural gas and electricity specific costs were assumed to be EUR 1.00 Nm<sup>−3</sup> and EUR 0.20 kWh<sup>−1</sup>, respectively.

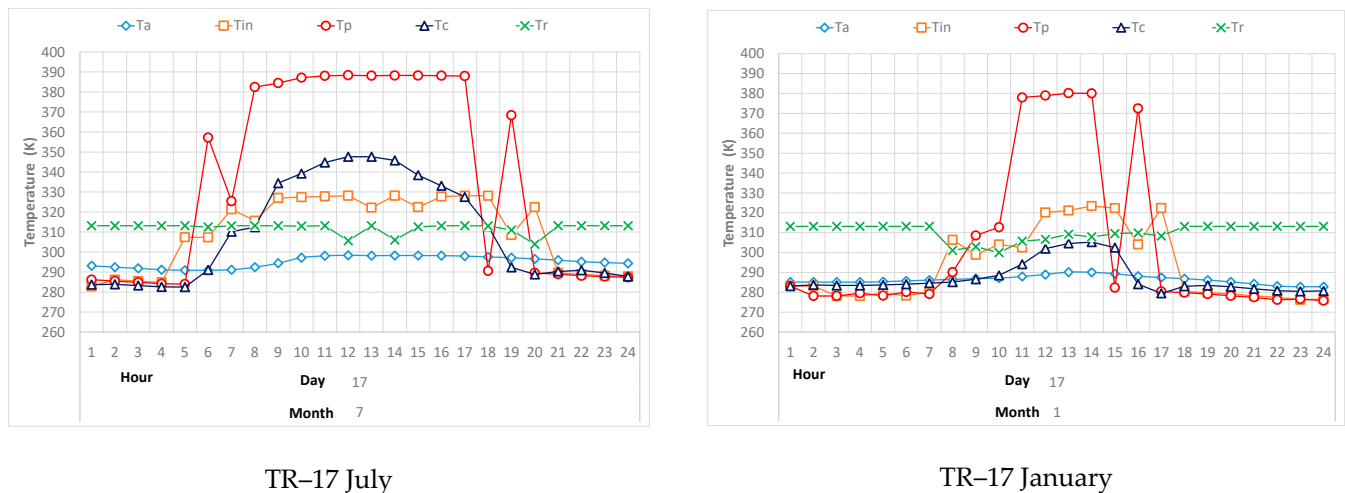
### 3. Results and Discussion

In this section, the main results of the energy, CO<sub>2</sub> emission and economic analysis for the two climates are reported.

#### 3.1. Energy Analysis

As a first step, the main temperatures of the glass covered PVT–RC module during a typical 24 h period were investigated, based on the validated mathematic model cited in previous Sections 2 and 3. Figure 5 refers to the TR climate. The initial water temperature in the tank was fixed at 10 °C at the simulation starting time, whereas the specific water

flow in the primary (collector) circuit was set to  $0.017 \text{ kg s}^{-1} \text{ m}^{-2}$  ( $60 \text{ kg h}^{-1} \text{ m}^{-2}$ ). Two 24 h periods in two different seasons were considered (17 January and 17 July) and the evaluation is reported in terms of the temperature of the glass cover  $T_c$  and of the collector plate  $T_p$ , together with the air temperature  $T_a$ , collector inlet water temperature  $T_{in}$  and heat exchanger return water temperature  $T_r$  (see also Figure 4).



TR-17 July

TR-17 January

**Figure 5.** Temperature of the cover ( $T_c$ ), plate collector ( $T_p$ ), outdoor air ( $T_a$ ), collector inlet ( $T_{in}$ ) and water return from the loads ( $T_r$ ) for the glass PVT-RC configuration (climate of Trapani).

As shown in Figure 5, the ambient air temperature in the hot and dry climate of Trapani remained relatively stable at around  $20^\circ\text{C}$  during night-time and  $25^\circ\text{C}$  during daytime in July ( $11^\circ\text{C}$  and  $16^\circ\text{C}$  respectively, in January). In Milano, the corresponding figures were  $23^\circ\text{C}$  during night-time and  $27^\circ\text{C}$  during daytime in July ( $3^\circ\text{C}$  and  $6^\circ\text{C}$  in January, respectively). Instead, the wind velocity fluctuated significantly with an average value of about  $2.8 \text{ m s}^{-1}$  in July and  $12.6 \text{ m s}^{-1}$  in January in TR ( $1.7 \text{ m s}^{-1}$  in July and  $1.5 \text{ m s}^{-1}$  in January in MI).

Due to the radiative sky cooling, the temperatures of both the glass cover and the plate were lower than the ambient temperature by several degrees in July. Consequently, the temperature of the PVT-RC module varied during the night. In the climate of Trapani, the temperature of the glass cover reduced averagely by  $3.5^\circ\text{C}$  as it was the thermal emitter of the PVT-RC module, thus exchanging heat to the sky. Indirect heat exchange through radiation to the glass cover allowed the plate to decrease its temperature by around  $2^\circ\text{C}$ . Moreover, by using a low-density polyethylene film as a transparent cover instead of glass, the temperature of the plate decreased during the night by around  $5^\circ\text{C}$  and it was averagely lower than the ambient temperature by  $13^\circ\text{C}$ , compared to  $6^\circ\text{C}$  obtained with a glass cover. This is due to the transparency of the former in the RC band. In the climate of Milano, such values were lower, due to the lower clearness of the sky.

A PVT module showed only a slightly higher  $T_p$  with respect to PVT-RC, in the order of  $4^\circ\text{C}$  in both climates; as a matter of fact, a typical PVT module, without any structural modification, exhibits an additional, not negligible cooling potential during the night-time which can be suitably used.

The monthly electricity, heat and cooling energy gained by the different solutions were determined by accumulating the daily energy gains. We can see, from Figure 6, that the maximum electricity ( $E_{PVT}$ ) and thermal energy ( $Q_{out,heat}$ ) were achieved in June and July, respectively, for all cases. This is due to the greatest total solar irradiance received in June with a lower average air temperature with respect to July, thus causing greater electrical efficiency in June and a better thermal efficiency in July. For the Trapani climate, the values ranged from  $25.6 \text{ kWh m}^{-2}$  for the glass PVT-RC to  $30.6 \text{ kWh m}^{-2}$  for the polyethylene PVT for  $E_{PVT}$  and from  $55 \text{ kWh m}^{-2}$  for the polyethylene PVT to

111.1 kWh m<sup>-2</sup> for the glass PVT-RC for  $Q_{out,heat}$ . For the climate of Milano, the same figures were lower for  $E_{PVT}$  (21.2 and 25.9 kWh m<sup>-2</sup>, respectively), but greater for  $Q_{out,heat}$  (60.8 and 119.1 kWh m<sup>-2</sup>, respectively).

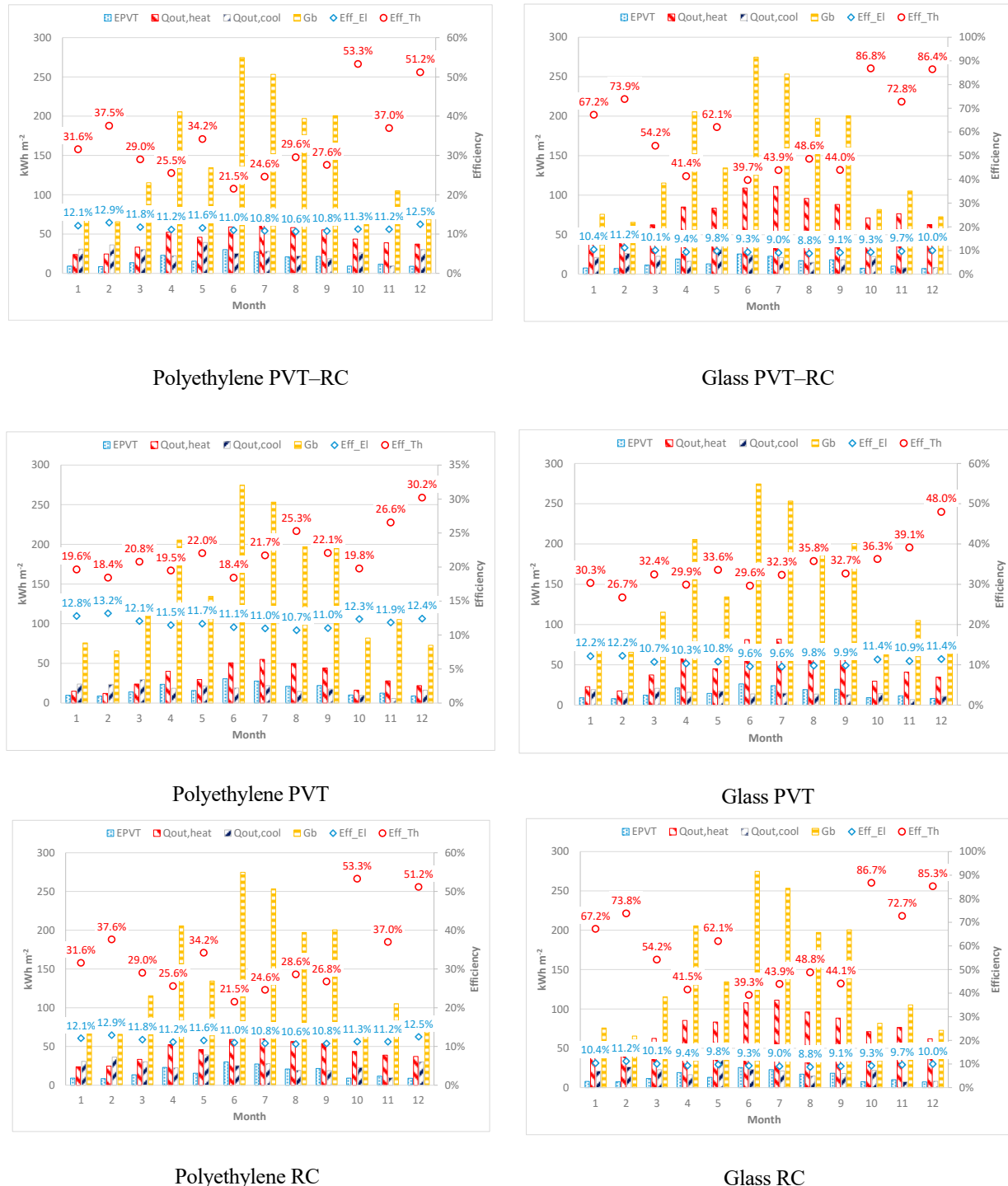


**Figure 6.** Monthly energy production (electricity ( $E_{PVT}$ ), thermal energy ( $Q_{out,heat}$ ) and cooling energy ( $Q_{out,cool}$ )), solar radiation ( $G_{\beta}$ ), thermal and electrical efficiency (Eff\_Th and Eff\_EI) for the different solutions (40 mm insulation thickness) in TR.

However, the minimum electricity and heat outputs were in January for all solutions (14.9 kWh m<sup>-2</sup> for the polyethylene PVT for thermal energy and 7.9 kWh m<sup>-2</sup> for the glass PVT-RC for electricity in Trapani), due to the lowest value of total solar irradiance. Note

that, in the climate of Milano, the polyethylene cover was not a viable solution as the useful thermal energy produced by the collector was zero or near zero in December and January.

For the night-time cooling performance, the monthly cooling energy gradually decreased from January to July and then increased during the other months of the year. The plant produced the highest monthly cooling energy in winter: 30.5 kWh m<sup>-2</sup> for the polyethylene PVT–RC system in December and around 20 kWh m<sup>-2</sup> for the glass PVT system in January for Trapani; 37.7 kWh m<sup>-2</sup> for the polyethylene PVT–RC system in January and 18 kWh m<sup>-2</sup> for the glass PVT system in November for Milano. Instead, the lowest monthly cooling energy was produced in summer (22.2 kWh m<sup>-2</sup> and 13.8 kWh m<sup>-2</sup> in August, respectively, for Trapani, whereas, in Milano, the lower clearness of the sky caused a further 10% lower value).

As a first conclusion, the system can provide considerable cooling energy during summer that allowed all the configurations simulated to cover the whole cooling load of the building in a passive and environment-friendly manner. Only the glass PVT solution in Trapani did not cover the whole cooling load (87.6%). Moreover, introducing an energy storage component, such as phase-change material (PCM), could be a viable solution both in the long-term (cooling energy in winter could be reserved for use during the following summer [35]) and in the short-term (the PCM could be employed to save cooling energy in the night-time and release it for use the following day when cooling demands are greater [36]). Nevertheless, introducing a thermal storage would probably slightly affect the energy performance and the economic viability of the plant.

The effects of insulation thickness on the daytime and night-time performance of the glass PVT–RC system are investigated as well. The electrical, thermal and cooling specific energy production and electrical/thermal efficiencies for a greater insulation thickness (100 mm instead of 40 mm) are depicted in Figure 7 on the monthly basis for the climate of Trapani. The electrical efficiency decreased with the increase in insulation thickness, above all during summer. By contrast, the thermal efficiency improved with the increase in insulation thickness, above all in winter. A thicker insulation layer leads to lower heat loss and higher PV module temperature, thus enhancing the solar thermal efficiency while deteriorating the PV efficiency. A further increase in insulation layer thickness would have a lower marginal benefit in relative terms.

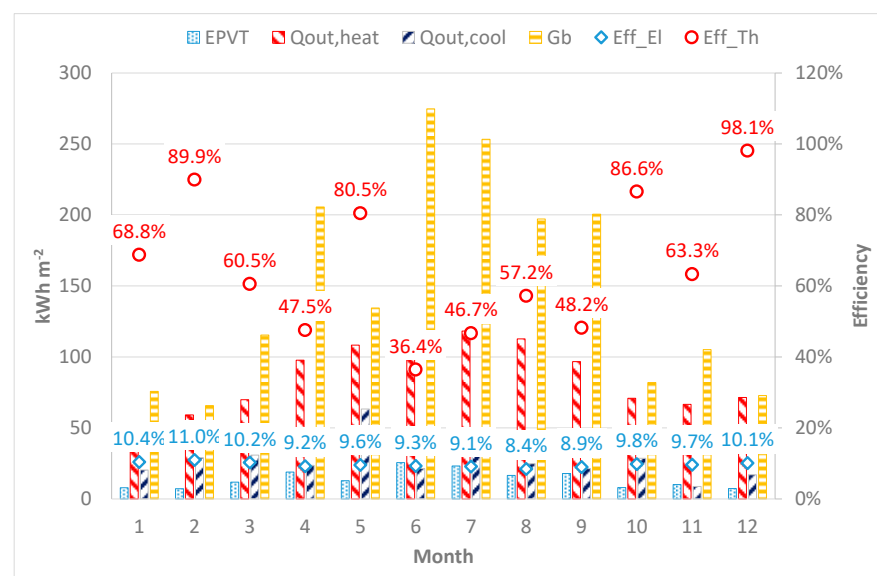


**Figure 7.** Monthly energy production (electricity ( $E_{PVT}$ ), thermal energy ( $Q_{out,heat}$ ) and cooling energy ( $Q_{out,cool}$ ), solar radiation ( $G_{\beta}$ ), thermal and electrical efficiency (Eff\_Th and Eff\_EI) for the glass PVT–RC solution with 100 mm insulation thickness (TR).

The 100 mm insulation layer suppressed the cooling loss of the glass PVT–RC system. Then, a higher cooling energy gain was determined, above all during summer. In relative terms, with an increase in insulation thickness from 0.04 m to 0.10 m, the cooling energy capacity increased much more in the hotter and dryer climate of Trapani (from 2419 kWh to 3201 kWh, that is, by 32%) than in Milano (from 3732 kWh to 4234 kWh, that is by 13%).

Electrical, thermal and cooling energy gains of the different systems are reported in Table 2 in terms of annual performance. The last three rows of the table report the load factors. If the solutions are compared on the basis of electricity production, the polyethylene PVT collector is the best one (2049 kWh in TR and 1554 kWh in MI, with an annual average electrical efficiency of around 11.5% in both climates). Instead, if the comparison is made on the basis of thermal energy, the glass PVT–RC showed the best performance, even with an increased insulation thickness. If the comparison is based on the useful thermal energy produced yearly, the hotter and dryer climate of Trapani features the best performance (10,238 kWh in TR and 9740 kWh in MI). Instead, in terms of thermal efficiency, Milano shows the best performance (57.4% in TR and 73% in MI). As a result, the lass PVT–RC with a thicker insulation layer is the best solution in terms of both overall efficiency (electric + thermal) and cooling energy capacity (3200 kWh in TR, slightly better than the polyethylene RC collector; 4324 kWh in MI, definitely better than the polyethylene RC).

A further comparison can be conducted based on the non-renewable primary energy (*PE*) consumed to satisfy the (eventual) parts of the loads not fully covered by the collectors and on the primary energy saving (*PES*) related to a reference plant configuration. As reported in Figure 8, the best solutions are the polyethylene PVT–RC and polyethylene RC in TR, whereas they are the glass PVT–RC in MI. They are the configurations that allow the best electrical and thermal energy load factors to be obtained. They both had a *PES* greater than 95% in TR and around 70% in MI. The *PE* consumption of the best configurations was around 500 kWh in TR and 5370 kWh in MI (4216 kWh with increased insulation thickness). Instead, the collector with polyethylene cover and PVT plate spectral emissivity featured the worst performance in terms of *PE* (1950 kWh in TR and 10,563 kWh in MI) and *PES* (82.8% in TR and 38.8% in MI). Moreover, it is interesting to note that the typical PVT module had a performance quite similar to the best ones in the climate of Trapani (it featured a *PE* consumption of 700 kWh and a *PES* of 93.8%), whereas it was quite penalized in the colder and more humid climate of Milano (*PE* 9150 kWh and *PES* 47%).

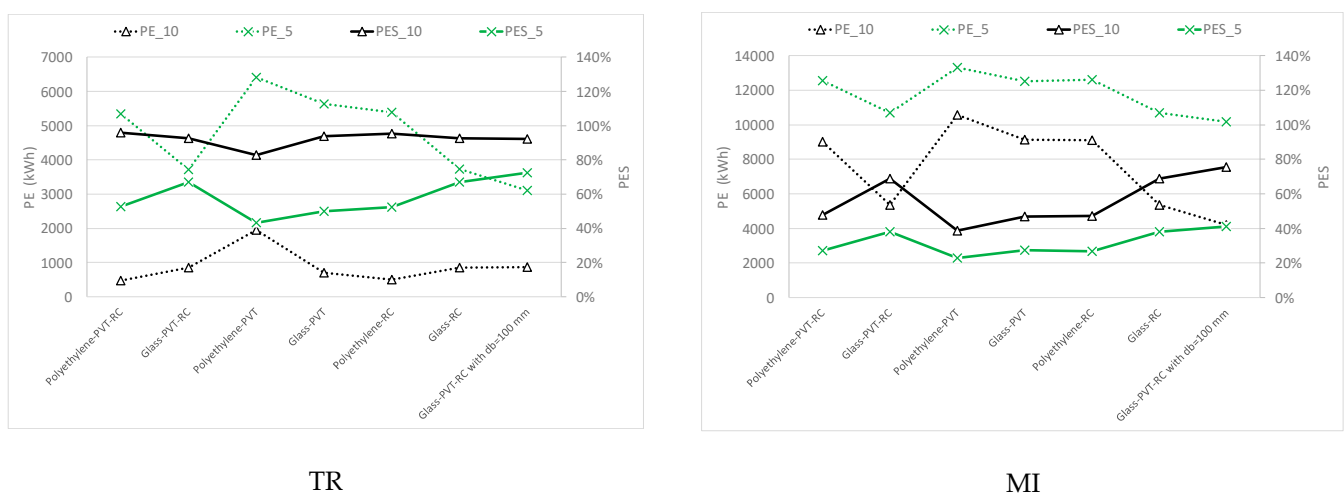


**Figure 8.** Annual *PE* consumption of the plant configurations tested in this study and *PES* with respect to the reference plant configuration as described in Section 2.4.

**Table 2.** Annual results in terms of energy production, efficiency and load factors.

		Trapani							Milano						
		Polyethylene PVT-RC	Glass PVT-RC	Polyethylene PVT	Glass PVT	Polyethylene RC	Glass RC	Glass PVT-RC *	Polyethylene PVT-RC	Glass PVT-RC	Poly Ethylene-PVT	Glass PVT	Poly Ethylene-RC	Glass RC	Glass PVT-RC *
$E_{PVT}$	kWh	2003	1686	2049	1844	2002	1685	1676	1518	1296	1554	1397	1518	1295	1272
$Q_{out,heat}$	kWh	5355	9455	3865	5897	5320	9443	10,238	4716	8600	3176	4812	4615	8598	9740
$Q_{out,cool}$	kWh	3200	2419	2219	1760	3144	2392	3201	4021	3732	2895	1930	3870	3715	4234
$G_{\beta}$	kWh	17,827	17,827	17,827	17,827	17,827	17,827	17,827	13,348	13,348	13,348	13,348	13,348	13,348	13,348
$\eta_{el}$		11.2%	9.5%	11.5%	10.3%	11.2%	9.5%	9.4%	11.4%	9.7%	11.6%	10.5%	11.4%	9.7%	9.5%
$\eta_{th}$		30.0%	53.0%	21.7%	33.1%	29.8%	53.0%	57.4%	35.3%	64.4%	23.8%	36.1%	34.6%	64.4%	73.0%
$E_{load}$	kWh	2121	2121	2121	2121	2121	2121	2121	2121	2121	2121	2121	2121	2121	2121
$Q_{heating + DHW}$	kWh	5586	5586	5586	5586	5586	5586	5586	12,179	12,179	12,179	12,179	12,179	12,179	12,179
$Q_{cooling}$	kWh	2008	2008	2008	2008	2008	2008	2008	505	505	505	505	505	505	505
$LF_{el}$		94.4%	79.5%	96.6%	87.0%	94.4%	79.5%	79.0%	71.6%	61.1%	73.3%	65.9%	71.6%	61.0%	60.0%
$LF_{heat}$		95.9%	100.0%	69.2%	100.0%	95.2%	100.0%	100.0%	38.7%	70.6%	26.1%	39.5%	37.9%	70.6%	80.0%
$LF_{cool}$		100.0%	100.0%	100.0%	87.6%	100.0%	100.0%	100.0%	100.0%	100.0%	100.0%	100.0%	100.0%	100.0%	100.0%

\* With  $d_b = 100$  mm.

An increase in solar collector's area would indeed increase the *PES* and reduce the *PE* consumption; the same solutions as the ones described above would be the best ones. Instead, Figure 8 reveals that a decrease in the collector's area (from 10 to 5 m<sup>2</sup>) would make the glass PVT-RC solution the most effective one (even with a thicker insulation layer), also in the climate of Trapani.

As a final remark, the energy required to pump the working fluid in the PVT system is not accounted for in the energy and (following) economic analyses. As a matter of fact, based on the previous literature and experience of the Authors [37,38], the auxiliary equipment electricity consumption (pumps of the PVT circuit) is not negligible at all in case of multisource heat pump systems with ground and solar energy as cold source of the heat pump. In this case, it can weigh up to 10% of the primary energy consumed by the plant. Instead, in the case of PVT only, as in this study, the weight of the auxiliary energy required to power the solar pump is typically around 3–5%.

### 3.2. Environmental Analysis

In terms of global warming impact, the monthly CO<sub>2</sub> emission savings of the glass PVT-RC configuration are depicted in Figure 9. Throughout the whole year, the greater part of the emission savings is due to the thermal energy produced by the collector for DHW and heating, above all for the climate of Trapani. Savings due to the electricity production assume a relevant value mainly during the summer months.

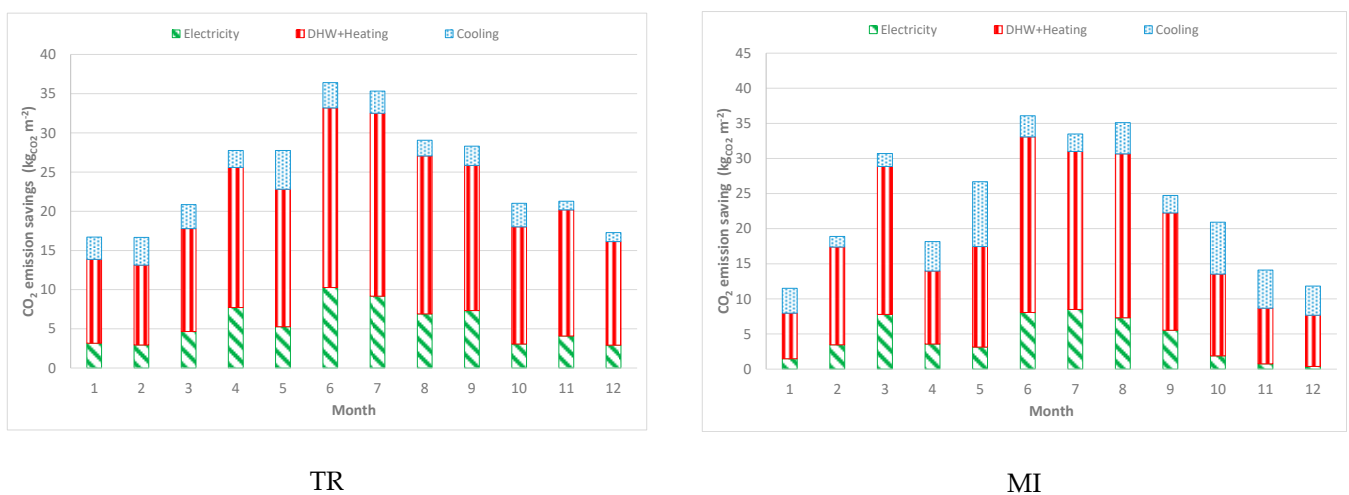


**Figure 9.** Monthly CO<sub>2</sub> emission savings in specific terms (i.e., per m<sup>2</sup> of collector area) for the glass PVT-RC configuration with respect to the traditional configuration plant.

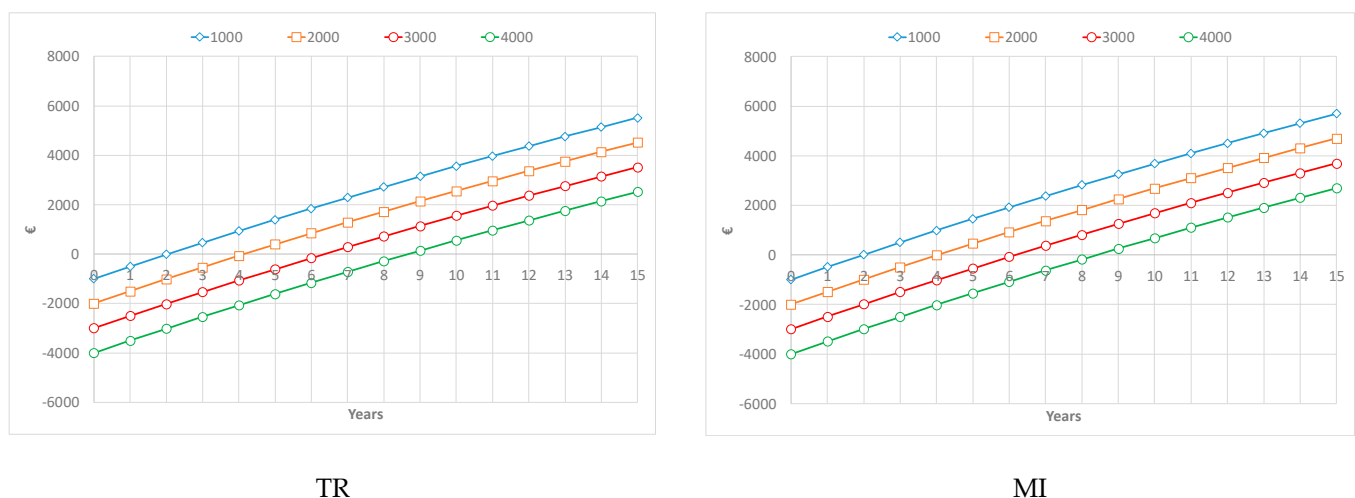
The different configurations are compared in terms of emission savings with respect to the traditional solution in Table 3. Again, the glass PVT-RC, even with a thicker insulation layer, features the best performance. It is worth noting the remarkable environmental benefit of this solution, due to the superiority of the *PES* compared to the others and the different CO<sub>2</sub> emission rates for natural gas and electrical energy.

**Table 3.** CO<sub>2</sub> specific emission savings of the different configurations with respect to the traditional configuration plant (values in kg<sub>CO2</sub> m<sup>-2</sup>).

		Poly Ethylene-PVT-RC	Glass PVT-RC	Poly Ethylene-PVT	Glass PVT	Poly Ethylene-RC	Glass RC	Glass PVT-RC with $d_b = 100$ mm
TR	Electricity	80.1	67.4	81.9	73.8	80.1	67.4	67.0
	DHW + heating	112.5	198.6	81.2	123.9	111.8	198.4	215.1
	Cooling	42.7	32.2	29.6	23.5	41.9	31.9	42.7
	Total	235.3	298.3	192.7	221.1	233.8	297.7	324.8
MI	Electricity	60.7	51.8	62.1	55.9	60.7	51.8	50.9
	DHW + heating	115.5	198.8	84.5	122.3	113.4	198.7	220.9
	Cooling	45.1	42.8	31.3	21.6	43.1	42.6	47.8
	Total	221.3	293.4	177.9	199.7	217.2	293.1	319.6

### 3.3. Economic Analysis

The energy convenience of a technical solution does not always correspond to economic advantage; moreover, the latter is often considered more important than the former. For this reason, an economic analysis of the best configuration based on the previous energy analysis was carried out. Figure 10 reports the cumulative differential cash flows of the glass PVT-RC configuration with respect to the reference plant. In the latter, the thermal energy, the cooling energy and the electrical energy produced by the collector were supposed to be provided, respectively, by natural gas feeding a condensing boiler and electricity from the grid to feed the air–water compression chiller and to face the electricity load. Natural gas, electricity from the grid and the extra-investment of glass PVT-RC collector are valorized with the values reported in Section 2.4.

**Figure 10.** Cumulative differential cash flows for the glass PVT-RC configuration with respect to the traditional plant for the two climates analyzed.

The y axis zero-cross point in Figure 10 represents the *DPP* of each case (different values of the extra-investment of the glass PVT-RC collector), whereas the value of the curves at the end of the 15 years period of the analyses represents the *NPW*. The economic analysis of the two climates exhibits very similar results, in terms of both *DPP* (varying between 2 and 8.7 years) and *NPW* (from EUR 2520 to EUR 5520). In fact, in the hotter climate of TR, the lower savings in natural gas related to MI are substantially compensated by the greater saving in electricity from the grid.

#### 4. Conclusions

The study here reported investigates numerically different configurations of a hybrid PVT–RC system based on a mathematical model, which was previously validated against experimental data. The annual energy, CO<sub>2</sub> emissions and economic sustainability of the system are analyzed in two typical Mediterranean climates on the basis of the test reference years. The results of the annual performance investigation of the best performing configuration (glass PVT–RC) suggest that the maximum and the minimum heat gain were obtained in July and February, respectively (1111 kWh and 486 kWh for the hotter and dryer climate; 1191 kWh and 309 kWh, respectively, for the milder and more humid one). The maximum (306 kWh in TR and 259 kWh in MI) and minimum (87 kWh in TR and 11 kWh in MI) electricity production for the most effective solution (polyethylene PVT) were obtained in June for TR (July for MI) and February for TR (December for MI), respectively. The peak and lowest cooling gains of the system are expected, for TR, in May and November, reaching 393 kWh and 97 kWh for the polyethylene PVT–RC solution, respectively. For MI, the corresponding figures are 594 kWh and 109 kWh in May and February, respectively.

For both climates, the glass PVT–RC is the best solution in terms of both overall efficiency (electric + thermal) and cooling energy capacity, even better if arranged with a thicker insulation layer. Nevertheless, the typical glass PVT module achieves a performance quite similar to the best ones.

In summary, the proposed glass PVT–RC collector can cover a great part of the energy load in an environment-friendly manner by coupling the collector with the inherent heating, ventilation and air conditioning system in buildings. A typical glass PVT collector can also serve in this scope with an interesting primary energy saving. As a further development of this study, a more comprehensive analysis will be developed by considering a multisource renewable-based plant, e.g., equipped with a multisource heat pump, in different climates to evaluate the effect of the latter on the performance of the system.

**Author Contributions:** Conceptualization, M.N.; methodology, M.N., S.M. and R.R.; software, M.N.; validation, M.N., S.M. and R.R.; writing—original draft preparation, M.N.; writing—review and editing, M.N., S.M. and R.R. All authors have read and agreed to the published version of the manuscript.

**Funding:** This research received no external funding.

**Institutional Review Board Statement:** Not applicable.

**Informed Consent Statement:** Not applicable.

**Conflicts of Interest:** The authors declare no conflict of interest.

#### Nomenclature

##### Acronyms

DHW	domestic hot water
MI	Milano
NZEB	nearly zero-energy building
PV	photovoltaic
PVT	photovoltaic/Thermal
RC	radiative cooling
SH	solar heating
TR	Trapani

## Symbols

$B_r$	temperature coefficient of the solar cells ( $K^{-1}$ )
$DCF$	discounted cash flow (EUR)
$DPP$	discounted payback period (y)
$d_{p,c}$	distance cover-plate (mm)
$d_b$	insulation thickness (mm)
$k_b$	insulation thermal conductivity ( $W m^{-1} K^{-1}$ )
$E_{b,\lambda}$	spectral radiation power ( $W m^{-2} \mu m^{-1}$ )
$E_{load}$	electric load (kWh, $kWh m^{-2}$ )
$E_{PVT}$	electric energy produced by the collector (kWh, $kWh m^{-2}$ )
$f_{p,ren}$	non-renewable primary energy factor
$G_\beta$	global solar radiation on the collector surface (kWh, $kWh m^{-2}$ )
$LF_{cool}$	cooling load factor
$LF_{el}$	electricity load factor
$LF_{heat}$	heating load factor
$m_p$	primary circuit specific mass flow rate ( $kg h^{-1} m^{-2}$ )
$m_s$	secondary circuit specific mass flow rate ( $kg h^{-1} m^{-2}$ )
$NPW$	net present worth (EUR)
$P$	extra-investment of the trigeneration with respect traditional plant (EUR)
$PE$	primary energy (kWh)
$PES$	primary energy Saving
$Q_{cooling}$	cooling load (kWh, $kWh m^{-2}$ )
$Q_{heating}$	heating load (kWh, $kWh m^{-2}$ )
$Q_{heating + DHW}$	heating + DHW load (kWh, $kWh m^{-2}$ )
$Q_{out,cool}$	cooling energy produced by the collector (kWh, $kWh m^{-2}$ )
$Q_{out,heat}$	thermal energy produced by the collector (kWh, $kWh m^{-2}$ )
$S$	annual saving (EUR $y^{-1}$ )
$t$	year
$T_a$	outdoor air temperature ( $^{\circ}C$ )
$T_c$	cover temperature ( $^{\circ}C$ )
$T_{in}$	inlet temperature ( $^{\circ}C$ )
$T_p$	plate temperature ( $^{\circ}C$ )
$T_r$	return temperature ( $^{\circ}C$ )
$\epsilon$	efficiency of the heat exchanger
$\epsilon_c$	emissivity of the cover
$\epsilon_p$	emissivity of the plate
$\eta_{el}$	electrical efficiency of the collector
$\eta_{el,sp}$	electrical efficiency of the separate production
$\eta_{th}$	thermal efficiency of the collector
$\eta_{th,sp}$	thermal efficiency of the separate production
$\eta_{ref}$	reference electrical efficiency of the solar cells
$\rho_c$	reflectance of the cover
$\rho_p$	reflectance of the plate
$\tau_c$	transmittance of the cover

## References

1. Lazzarin, R. Heat pumps and solar energy: A review with some insights in the future. *Int. J. Refrig.* **2020**, *116*, 146–160. [CrossRef]
2. Lazzarin, R. Renewable energy technologies in air conditioning: State-of-the-art and perspectives. In Proceedings of the 25th IIR International Congress of Refrigeration, Montréal, QC, Canada, 24–30 August 2019; pp. 130–141.
3. IEA. *World Energy Outlook 2020*; IEA: Paris, France, 2020; Available online: <https://www.iea.org/reports/world-energy-outlook-2020> (accessed on 1 September 2021).
4. Fraunhofer Institute for Solar Energy Systems. Photovoltaics Report. 2021. Available online: <https://www.ise.fraunhofer.de/content/dam/ise/de/documents/publications/studies/Photovoltaics-Report.pdf> (accessed on 1 September 2021).
5. Yang, H.; Wang, Q.; Huang, X.; Li, J.; Pei, G. Performance study and comparative analysis of traditional and double-selective-coated parabolic trough receivers. *Energy* **2017**, *145*, 206–216. [CrossRef]

6. Dan, A.; Barshilia, H.C.; Chattopadhyay, K.; Basu, B. Solar energy absorption mediated by surface plasma polaritons in spectrally selective dielectric-metaldielectric coatings: A critical review. *Renew. Sustain. Energy Rev.* **2017**, *79*, 1050–1077. [[CrossRef](#)]
7. Ning, Y.; Wang, W.; Wang, L.; Sun, Y.; Song, P.; Man, H.; Zhang, Y.; Dai, B.; Zhang, J.; Wang, C.; et al. Optical simulation and preparation of novel Mo/ZrSiN/ZrSiON/SiO<sub>2</sub> solar selective absorbing coating. *Sol. Energy Mater. Sol. Cell* **2017**, *167*, 178–183. [[CrossRef](#)]
8. Bauer, G.H. *Photovoltaic Solar Energy Conversion*; Springer: Berlin/Heidelberg, Germany, 2015; ISBN 978-3-662-46683-4.
9. Theodore, L. *Heat Transfer Applications for the Practicing Engineer*; John Wiley & Sons: Hoboken, NJ, USA, 2011.
10. Chow, T.T. A review on photovoltaic/thermal hybrid solar technology. *Appl. Energy* **2010**, *87*, 365–379. [[CrossRef](#)]
11. REN 21. Renewables 2020—Global Status Report. Available online: <https://www.ren21.net/gsr-2020/> (accessed on 2 September 2021).
12. Montagnino, F.M. Solar cooling technologies. Design, application and performance of existing projects. *Sol. Energy* **2017**, *154*, 144–157. [[CrossRef](#)]
13. Lazzarin, R.; Noro, M. Past, present, future of solar cooling: Technical and economical considerations. *Sol. Energy* **2018**, *172*, 2–13. [[CrossRef](#)]
14. Lazzarin, R.; Noro, M. Heating and Cooling of a Building by Absorption Heat Pumps driven by Evacuated Tube Solar Collectors (ETCs). In Proceedings of the ISHPC 2021 Proceedings—Online Pre-Conference 2020, Berlin, Germany, 22–25 August 2021; pp. 133–136. [[CrossRef](#)]
15. Noro, M.; Lazzarin, R. PVT and ETC Coupling for Annual Heating and Cooling by Absorption Heat Pumps. *Sustainability* **2020**, *12*, 7042. [[CrossRef](#)]
16. Raman, A.P.; Anoma, M.A.; Zhu, L.; Rephaeli, E.; Fan, S. Passive radiative cooling below ambient air temperature under direct sunlight. *Nature* **2014**, *515*, 540–544. [[CrossRef](#)]
17. Zhai, Y.; Ma, Y.; David, S.N.; Zhao, D.; Lou, R.; Tan, G.; Yang, R.; Yin, X. Scalable-manufactured randomized glass-polymer hybrid metamaterial for daytime radiative cooling. *Science* **2017**, *355*, 1062–1066. [[CrossRef](#)] [[PubMed](#)]
18. Vall, S.; Castell, A. Radiative cooling as low-grade energy source: A literature review. *Renew. Sustain. Energy Rev.* **2017**, *77*, 803–820. [[CrossRef](#)]
19. Gentle, A.R.; Smith, G.B. A subambient open roof surface under the Mid-Summer sun. *Adv. Sci.* **2015**, *2*, 1500119. [[CrossRef](#)] [[PubMed](#)]
20. Kou, J.-L.; Jurado, Z.; Chen, Z.; Fan, S.; Minnich, A.J. Daytime radiative cooling using near-black infrared emitters. *ACS Photon.* **2017**, *4*, 626–630. [[CrossRef](#)]
21. Chen, J.; Lu, L. Development of radiative cooling and its integration with buildings: A comprehensive review. *Sol. Energy* **2020**, *212*, 125–151. [[CrossRef](#)]
22. Zhang, J.; Yuan, J.; Liu, J.; Zhou, Z.; Sui, J.; Xing, J.; Zuo, J. Cover shields for sub-ambient radiative cooling: A literature review. *Renew. Sustain. Energy Rev.* **2021**, *143*, 110959. [[CrossRef](#)]
23. Zhao, B.; Hu, M.; Ao, X.; Pei, G. Conceptual development of a building-integrated photovoltaic–radiative cooling system and preliminary performance analysis in Eastern China. *Appl. Energy* **2017**, *205*, 626–634. [[CrossRef](#)]
24. Hu, M.; Zhao, B.; Ao, X.; Zhao, P.; Su, Y.; Pei, G. Field investigation of a hybrid photovoltaic-photothermic-radiative cooling system. *Appl. Energy* **2018**, *231*, 288–300. [[CrossRef](#)]
25. Zhao, B.; Hu, M.; Ao, X.; Chen, N.; Pei, G. Radiative cooling: A review of fundamentals, materials, applications, and prospects. *Appl. Energy* **2019**, *236*, 489–513. [[CrossRef](#)]
26. Hu, M.; Su, Y.; Darkwa, J.; Riffat, S. Implementation of Passive Radiative Cooling Technology in Buildings: A Review. *Buildings* **2020**, *10*, 215.
27. Hu, M.; Zhao, B.; Ao, X.; Su, Y.; Wang, Y.; Pei, G. Comparative analysis of different surfaces for integrated solar heating and radiative cooling: A numerical study. *Energy* **2018**, *155*, 360–369. [[CrossRef](#)]
28. Hu, M.; Zhao, B.; Li, J.; Wang, Y.; Pei, G. Preliminary thermal analysis of a combined photovoltaic-photothermic-nocturnal radiative cooling system. *Energy* **2017**, *137*, 419–430. [[CrossRef](#)]
29. Hu, M.; Zhao, B.; Ao, X.; Ren, X.; Cao, J.; Wang, Q.; Su, Y.; Pei, G. Performance assessment of a trifunctional system integrating solar PV, solar thermal, and radiative sky cooling. *Appl. Energy* **2020**, *260*, 114167. [[CrossRef](#)]
30. Hu, M.; Zhao, B.; Ao, X.; Cao, J.; Wang, Q.; Riffat, S.; Su, Y.; Pei, G. An analytical study of the nocturnal radiative cooling potential of typical photovoltaic/thermal module. *Appl. Energy* **2020**, *277*, 115625. [[CrossRef](#)]
31. Vialetto, G.; Noro, M.; Rokni, M. Innovative household systems based on solid oxide fuel cells for the Mediterranean climate. *Int. J. Hydrogen Energy* **2015**, *40*, 14378–14391. [[CrossRef](#)]
32. CTI—Comitato Termotecnico Italiano. Weather Reference Year. Available online: <https://www.cti2000.it/index.php?controller=news&action=show&newsid=34985> (accessed on 15 July 2021). (In Italian)
33. Schibuola, L.; Tambani, C. Performance comparison of heat recovery systems to reduce viral contagion in indoor environments. *Appl. Therm. Eng.* **2021**, *190*, 116843. [[CrossRef](#)]
34. Noro, M.; Lazzarin, R.; Busato, F. Solar cooling and heating plants: An energy and economic analysis of liquid sensible vs phase change material (PCM) heat storage. *Int. J. Refrig.* **2014**, *39*, 104–116. [[CrossRef](#)]

35. Mancin, S.; Noro, M. Reversible Heat Pump Coupled with Ground Ice Storage for Annual Air Conditioning: An Energy Analysis. *Energies* **2020**, *13*, 6182. [[CrossRef](#)]
36. Righetti, G.; Lazzarin, R.; Noro, M.; Mancin, S. Phase Change Materials embedded in porous matrices for hybrid thermal energy storages: Experimental results and modelling. *Int. J. Refrig.* **2019**, *106*, 266–277. [[CrossRef](#)]
37. Lazzarin, R.; Noro, M. Lessons learned from long term monitoring of a multisource heat pump system. *Energy Build.* **2018**, *174*, 335–346. [[CrossRef](#)]
38. Lazzarin, R.; Noro, M. Photovoltaic/Thermal (PV/T)/ground dual source heat pump: Optimum energy and economic sizing based on performance analysis. *Energy Build.* **2020**, *211*, 109800. [[CrossRef](#)]